The Influence of Defects on the Reactivity of Organic Surfaces

Gregory J. Deye[†], Juvinch R. Vicente[‡], Jixin Chen[‡], Jacob W. Ciszek*[,†]

[†] Department of Chemistry and Biochemistry, Loyola University Chicago, 1032 West Sheridan Road, Chicago, Illinois, 60660, United States

[‡] Department of Chemistry and Biochemistry, Ohio University, 100 University Terrace, Athens, Ohio, 45701, United States

*jciszek@luc.edu

ABSTRACT

Molecular orientation within organic solids limits the range of applicable surface reactions, with reactive functionalities often recessed and inaccessible to adsorbates. To induce reactivity in heretofore inert orientations of acenes, a defect-mediated mechanism is utilized to functionalize thin-film phase pentacene. This mechanism was demonstrated via correlation of reaction data to defect density, determined via polarization modulation infrared reflection absorption spectroscopy (PM-IRRAS) and atomic force microscopy (AFM), respectively. By controllably varying the amount of grain boundaries in the acene films, the reaction can be varied from near zero to coverage exceeding a monolayer. The extensive coverage suggests the reaction propagates from the defects throughout the grains, a prediction borne out via direct observation of reaction progression along the surface from a single dislocation (via scanning electron microscopy). The results support a mechanism whereby the reaction is initialized at the defect sites, especially boundaries of crystal domains, which opens the unfavorable molecular orientation of the (001)

pentacene to incoming adsorbates. This exact film configuration and its successful reaction is especially relevant to organic thin-film transistor (OTFT) devices.

INTRODUCTION

Before organic films are adopted into optoelectronic devices, interfacial flaws like poor adhesion and charge injection barriers must first be addressed.[1-6] Of the available methods to improve the organic surface, the Diels-Alder reaction is an elegant solution because the π-electron rich molecules are primed for chemistry with electron deficient adsorbates. This reaction has been demonstrated with the prototypical semiconductor pentacene, [5,6] however, molecular orientation within the film limits the range and applicability of the reaction. Here, the ideal orientation for pentacene is a facedown configuration on the substrate where the reactive π-system is exposed to approaching adsorbates (Figure 1, left). The most common (and less ideal) configuration is where molecules orient ~68° from the surface in the thin-film phase.[7] In this orientation, the predominant crystal face exposed is the (001) face and, at the surface, only unreactive C-H bonds are presented to the adsorbates (Figure 1, right). In fact, when this is transposed to the unblemished surfaces of single crystals, the (001) facets have been demonstrated to be inert to Diels-Alder reaction conditions.[8] This bodes poorly for thin-film phase pentacene as the (001) surface forms the majority of the interface with deposited metals in top-contact organic thin-film transistors (OTFTs).

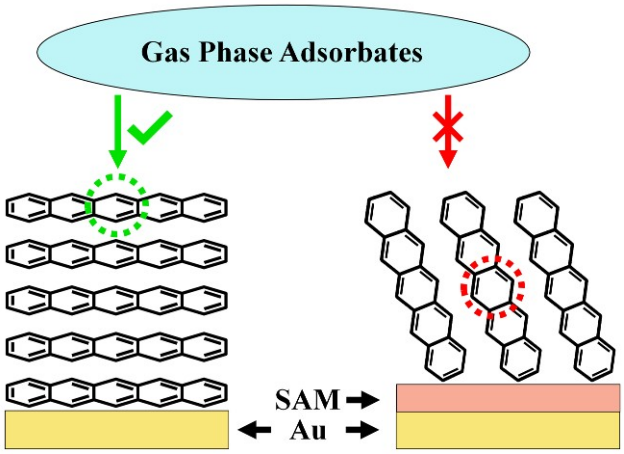

Figure 1. Highly orientation dependent access to reactive portions of pentacene thin films (dashed circles). (Left) Pentacene molecules on bare gold adopt a facedown configuration and adsorbates can freely approach the most reactive central ring for chemisorption. (Right) Pentacene on self-assembled monolayers (SAMs) adopts an upright configuration inhibiting adsorbate approach to any reactive π-system.

Fortunately, an unreactive crystal surface does not negate the possibility of reaction on thin films because structural defects (grain boundaries, dislocations, surface vacancies, step edges, and stacking faults) can have a profound influence on reactivity. Defects introduce a break in the crystallographic lattice, whether large in the case of grain boundaries, or atomic in the case of surface vacancies. When harnessed, defects can then trigger a broad collection of reactions. [9–14] For example, the dissociative chemisorption of small molecules (H_2O, CO, CO_2, SO_2, CH_3OH, CH_2CH_2) is facilitated via surface defects, specifically oxygen surface vacancies on metal oxides.[11,12] This defect mediated reactivity extends through metal chalcogenides [10,13] and other structures.[9,14] Though the mechanism would be dramatically different for organic surfaces (i.e. pentacene), the general prominence of defect-induced chemistry prompted us to examine if the

surface chemistry of organic films may also be influenced by defects and, if so, allow us to react a pentacene (001) surface.

As the defect density is very high in pentacene thin films, [15] if properly harnessed, defects have the potential to facilitate Diels-Alder functionalization. Defects produce structural discontinuities in the crystal lattice and these render the nearby molecules more reactive by expanding the surrounding void. [16,17] The formed voids in the film serve as potential loci for the adsorbate molecules to position themselves in the correct transition state geometry for reaction, and can also accelerate adsorbate diffusion into the film [18] to reach an unreacted portion of the molecular surface. These effects are likely amplified by the nature of the organic reaction: formation and buildup of product at the reacting surface induces strain and causes the formation of further defects which accelerates reaction propagation throughout the film or crystal. Strain induced propagation through organic crystals has some precedence in the form of self-rearrangement of oxime picryl ethers. [16] All told, the defect-mediated approach seems especially amenable to the reactivity of an organic film.

Herein, we examine the reaction of pentacene thin films with vapor phase adsorbates via Diels-Alder chemistry to study the defects associated with grain boundaries and their ability to initiate reactivity. Utilizing the substrate's temperature during pentacene film formation to alter average crystal grain size, we observe reactivity that is highly correlated. These results are then extended onto single crystal systems that are grown with one to two domain boundaries, where defect-induced reaction propagation can be observed. This defect-mediated mechanism demonstrates the viability of surface functionalization on heretofore unreactive surface orientations, and thus the viability of Diels-Alder chemistry towards improving OTFTs.

EXPERIMENTAL SECTION

Materials

All evaporation metals are of 99.9% or greater purity. Sublimed grade pentacene and tetracene, *N*-methylmaleimide, 1-dodecanethiol, and 200 proof ethanol (ACS grade) were commercially obtained and used without further purification.

Preparation of Gold Substrates

Rectangular cut Si(111) wafers were first cleaned in piranha solution (3:1, H_2SO_4: H_2O_2) for 30 min. The wafers were rinsed with copious amounts of 18 MΩ•cm water, sonicated for 20 min, and dried under a stream of nitrogen. Wafers were then mounted in a thermal evaporator (Kurt J. Lesker NANO38). A 5 nm chromium adhesion layer was deposited, followed by 50 nm of silver and 50 nm of gold at a base pressure of $<1\times10^{-6}$ Torr and a deposition rate of 1 Å/s.

Self-Assembly of 1-Dodecanethiol onto Gold Substrates

Self-assembled monolayer (SAM) decorated gold substrates were prepared by submerging the freshly prepared gold substrates in a nitrogen purged 200 proof ethanolic solution of ~1 mM 1-dodecanethiol for 24 h at room temperature. After the self-assembly, the substrates were rinsed with copious amounts of ethanol, sonicated, rinsed an additional time with ethanol, and dried under a stream of nitrogen. SAM thicknesses were assessed through ellipsometry measurements after the self-assembly (Gaertner Scientific LSE Stokes Ellipsometer with 632.8 nm laser). The surface thickness was modeled as a single absorbing layer atop an infinitely thick substrate (fixed n_s) and the index of refraction was set to 1.45. Following thickness measurements, the SAM substrates were carefully cut in half to generate a witness portion for microscopy, and a consumable portion

for reaction. Both parts were rinsed with ethanol, sonicated, rinsed again, and then dried under a stream of nitrogen.

Pentacene Thin Film Deposition

40 nm pentacene thin films were deposited using a home-built sublimation chamber, with a source to substrate distance of 16–17.5 cm, at a rate of 0.05 Å/s. Pentacene was sublimed from a resistively heated cartridge onto SAM decorated gold substrates at a base pressure of 2×10^{-6} Torr. During sublimation, the substrate temperature was controlled with a home-built resistive heating element which allowed a temperature differential to be maintained between two samples (Figure S1). Thicknesses of the films were monitored using a quartz crystal microbalance (INFICON SQM-160).

Measurement of Grain Structure

Witness samples were analyzed via atomic force microscopy (AFM; MFP 3D microscope, Asylum Research, Santa Barbara, CA, USA). AFM measurements were performed in tapping (noncontact) mode using a diamond-like-carbon coated AFM tip (Tap190DLC, Budget Sensors, Sofia, Bulgaria). The average grain size and total projected grain boundary length in each image was determined using AFM software (Gwyddion 2.5), whereby grains were marked by segmentation followed by measurements using 100 iterations of line-cut method.

Growth of Tetracene Crystals

Tetracene crystals were grown onto gold coated Si(111) substrates using a home-built physical vapor transport tube furnace that was 95 cm in length and had a temperature gradient of approximately ~2 °C/cm in the growth zone (Figure S2). [19] 100 mg of tetracene source material

were heated to 225 °C under a flow of ultra-high purity argon (40 mL/min). The crystals were collected from the region of the furnace at 205 °C after 48 h. The gold substrate with crystals was imaged before reaction with a Hitachi SU-3500 scanning electron microscope (SEM) at 5 kV.

Diels-Alder Reaction of Acene Surfaces

The acene samples and a small vial of approximately 8 mg of *N*-methylmaleimide were placed at opposite ends of a Schlenk tube under nitrogen. The samples were heated to 50 °C (pentacene films) or 80 °C (tetracene crystals) for 18 h. The reaction was quenched by insulating the substrate end of the Schlenk tube while cooling the opposite end with dry ice to condense residual *N*-methylmaleimide vapors. As an additional measure to remove physisorbed *N*-methylmaleimide, acene samples were further subjected to high vacuum conditions ($<5.5\times10^{-6}$ Torr) for at least 1 h. The extent of reaction on the thin films was evaluated by PM-IRRAS (Bruker Optics Tensor 37 with a PMA50 accessory and a liquid nitrogen cooled MCT detector). Spectra were taken at a resolution of 2 cm^{-1}. The extent of reaction on the surface was determined by the intensity of absorptions associated with adduct formation (1700 and 1280 cm^{-1}).[5] Reactions on crystal surfaces were qualitatively evaluated via comparison of SEM images before and after reaction.

RESULTS AND DISCUSSION

Defects are intrinsic to pentacene film growth and a tally of them is critical to forming an effective hypothesis concerning their role in reactivity. Typical pentacene thin films have on the order of 10^{11} dislocations/cm^2,[15] significantly more single vacancies,[20] and assuming an average grain size of about 500 nm, roughly 10^{8} grain boundaries per cm^{2}. All are expected to impact reactivity, as each provides a means for adsorbates to reach the recessed acene core (Figure 1,

right). While dislocations and vacancies are numerically attractive, they are challenging to control and thus they were not used to benchmark against reactivity. Though grain boundaries occur far less, their relative importance is outsized as this type of defect is large in size and also influences derivative defect (dislocation and vacancy) formation.[15,20–22] Indeed, grain boundaries are not reflective of merely being two domains meeting, but rather, the height change from edge to center implies additional step edges (roughly 30 for the films below). There is also a high degree of compressive stress at grain boundaries, and this interferes with ideal crystal geometry growth: dislocation formation is amplified under strain. [21] Due to both the ease with which they can be controlled, and their interrelationship with other defects, grain boundaries (and average grain size) are used to study how surface defects can impart reactivity to the thin-film phase of pentacene.

The average size of pentacene grains can be controlled via two methods: substrate control and thermal control. In the first method, self-assembled monolayers (SAMs) coat the underlying substrate and the SAM chain can control the nucleation density of the pentacene thin film. Longer SAMs have been hypothesized to generate significantly more nucleation sites for crystalline domains, resulting in smaller grains. [23] Several classes of SAMs have displayed this relationship between SAM chain length and pentacene grain size, including thiols, [24] silanes,[25,26] phosphonic acids,[27–29] and carboxylic acids.[30] In the second method, an elevated substrate temperature effectively lowers the activation energy for surface diffusion,[31,32] thereby allowing pentacene molecules to diffuse more rapidly on the surface and minimizing nucleation of new crystals.[33] This in turn facilitates the formation of larger crystalline grain sizes. Recent studies[34,35] have demonstrated a range of grain sizes of pentacene can be produced by controlling the temperature of the substrate during film formation.

Although there are several reports outlining the success of using SAMs as a means to control pentacene grain size, in our hands we found results to be highly varied. In contrast, thermally activated grain growth proved to be simple and robust. Grain size differentials were pronounced between the two different temperature samples, with nearly 425% larger average grain size when going from a substrate temperature of 30 to 60 ºC. The large difference in average grain size between the two temperature samples will greatly simplify the comparison between reactivity and defect density. Of additional merit, the batch to batch variability was low. At the temperatures evaluated, the average grain size varied by less than 100 nm (25%) between two sequential samples (Figure S3).

The aforementioned films were produced by depositing pentacene on 1-dodecanethiol coated gold substrates, a SAM being critical to generating thin-film phase pentacene.[7] The quality of the SAM was evaluated via surface order and thickness. The ν_{CHa} and ν_{CHs} peak positions in the IR spectra indicate the ordering of the alkane chain within the monolayer. These two peaks appear at 2920 and 2852 cm^{-1} for 1-dodecanethiol, respectively matching literature values within 2 cm^{-1} (Figure S4).[36] For ellipsometry, the thickness of the 1-dodecanethiol SAMs was 19 Å, which is consistent with previous reported thicknesses (18 Å).[37,38] Following pentacene deposition on the SAM, the orientation of pentacene was determined using the relative infrared peak intensities at 1445, 1164, 910, and 731 cm^{-1}; sets of vibrations that are orthogonal to one another. When pentacene within the film is oriented perpendicular to the gold surface (e.g. in a (001) film), the vibrations at 1445 and 1164 cm^{-1} are amplified while the normally dominant peaks at 910 and 731 are diminished[7] due to the surface selection rules.[39] IR spectra for the films are reported in Figure 2, and their IR absorptions confirm a nominally (001) film, i.e. the long axis of the pentacene is ~22º from the surface normal (Figure 1, right).

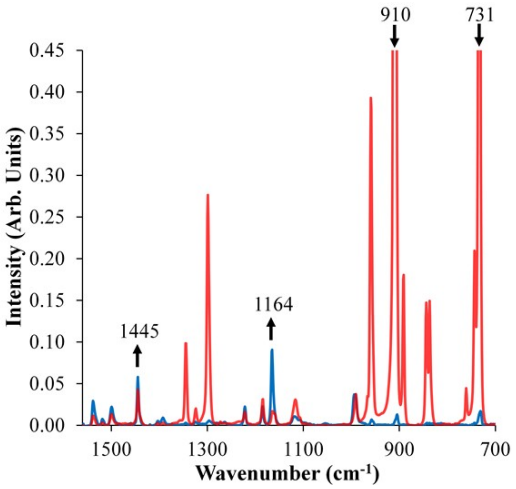

Figure 2. PM-IRRAS spectra of pentacene on bare gold (red; peaks are clipped for 910 and 731 cm^{-1}, but reach a maximum of 2.6 and 1.7 A.U.) and on 1-dodecanethiol (blue). Arrows at 1445, 1164, 910, and 731 cm^{-1} indicate the direction of the peak intensity change in going from pentacene on bare gold to a nominally (001) film.

AFM images (Figure 3) of the pentacene films reveal two very different grain sizes for the room temperature sample (400 ± 200 nm) and the one at elevated temperatures (1700 ± 800 nm for 60 °C), consistent with previously mentioned reports. [34,35] Further analysis of the AFM data (Figure 3c and d) indicates that the overall structure of each domain is similar, with rough terraces seen in both samples, and small vacancies (equivalent to ~2 nm thickness, or about two molecules of thickness) seen across the terraces. Because the average exposed area of the side surface is the length of the total grain boundary length times the film thickness, the total grain boundary length can be used to represent the average defect area of the films with the same thickness. For the samples in Figure 3, this is 226 ∝m vs 68 ∝m or a 3.3-fold difference. Since the defect density on the room temperature substrate is so markedly higher, if defects do play a critical role in reactivity, these two samples should have dramatically different reactivity; it also remains to be seen if the

defects in either sample are sufficient to render this surface reactive on the timescale of this experiment.

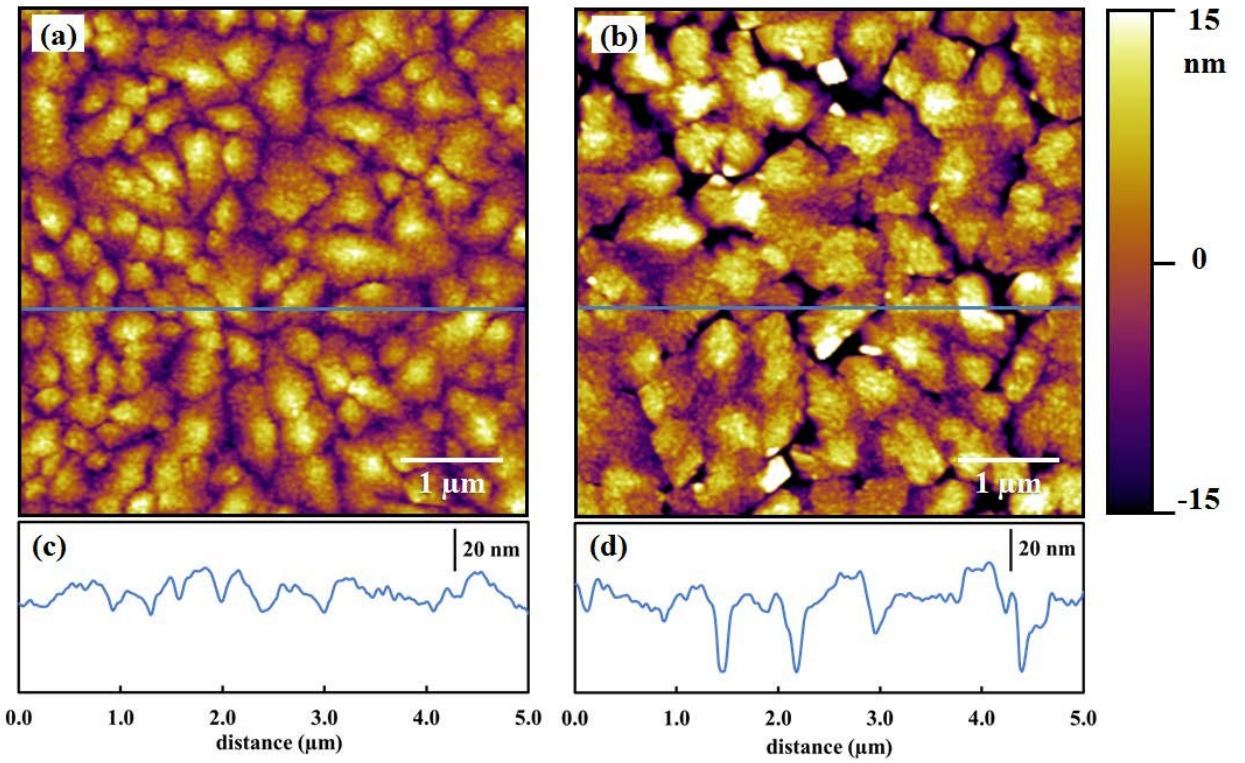

Figure 3. Grain structure of 40 to 50 nm thick pentacene thin films sublimed onto 1-dodecanethiol decorated gold substrates at a) room temperature and b) 60 °C. The AFM images (5×5 ∝m) were taken in non-contact mode. Line scans across the c) room temperature substrate and d) 60 °C substrate.

The reaction of pentacene films was accomplished by heating the substrate in the presence of vapor phase *N*-methylmaleimide for 18 h at 50 °C. IR analysis of these films reveals the growth of new infrared peaks at 1700 cm^{-1} and 1280 cm^{-1}. These peaks suggest that an effective Diels-Alder reaction has taken place on the pentacene film (Figure 4). It is remarkable that the pentacene (001) surface is reactive, and this will be discussed in further detail later. But the greater point is

that the reactivity of each film is highly correlated to the projected grain boundary length which demonstrates that the defects are the likely source of this reactivity. Specifically, the room temperature sample (boundary length = 226 ∝m) has reacted significantly faster than the 60 ºC sample (boundary length = 68 ∝m). While the data correlation appears semiquantitative, with a 3.3-fold increase in boundary length generating a 3 to 4-fold increase in reactivity, we caution against over quantifying the relationship as some samples had lower reactivity differences (Figure S5). However, when one considers the lack of reactivity in single crystal samples[8], a direct relationship is evident. Another aspect of this data is that peak intensities are near or above what would be expected for reacting a monolayer's worth of material with the pentacene film. This suggests that the reaction is not confined to the grain boundaries, rather, the boundaries act as a site from which reaction can propagate across the surface and into the subsurface.

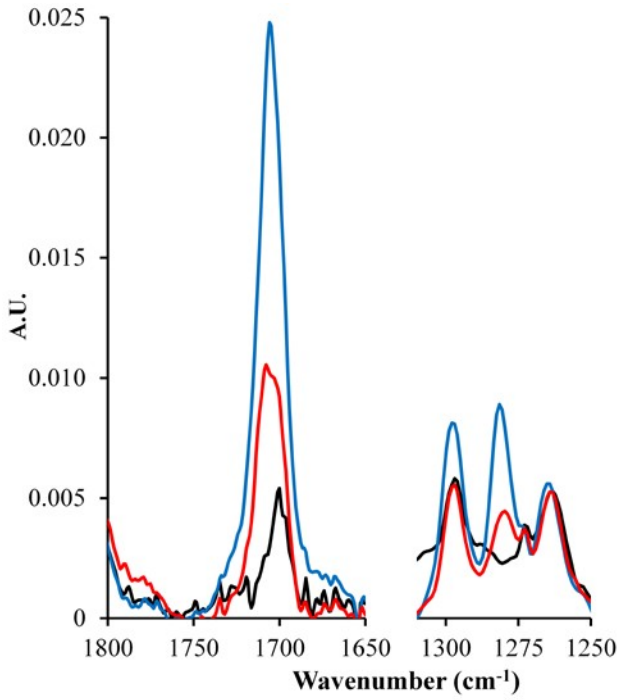

Figure 4. PM-IRRAS spectra comparing reactivity of pentacene films with *N*-methylmaleimide for 18 h at 50 °C. The color scheme is as follows: unreacted pentacene (black), reaction of

pentacene films prepared at 60 °C (red), and reaction of pentacene films prepared at room temperature (blue).

We wish to reemphasize the significance of being able to react the imperfect (001) pentacene surface. Previously, the exposure of tetracene crystals to Diels-Alder reaction conditions revealed the main face, (001), was unreactive. [8] In our work, with milder conditions, pentacene films with intrinsically high defect density resulted in significant reaction at the surface. More importantly, results showing monolayer or greater coverage implies that the reaction may be propagating across the surface. This relationship compelled us to examine if propagation from a small amount of defects could render the (001) surface of a *crystal* reactive. To explore this phenomenon more fully, and for direct evidence of this propagation, reaction on a surface that is predominantly defect-free is required.

Tetracene crystals were grown from the vapor phase in a manner similar to Laudise.[19] They are, on average, larger than 50 μm in size and have well-defined crystal faces. Scanning electron microscopy (SEM) was used to survey the crystals, and then locate crystals with only one or two significant defects on the surface. In Figure 5a, we isolated a single crystal with only one major defect on the surface: a line originating from the bottom of the hexagonal crystal and continuing through roughly a quarter of the crystal (indicated by arrows). If the propagation of adsorbates is indeed occurring, one should be able to observe its dispersal from this feature. This experiment is made simpler by the fact that reaction with *N*-methylmaleimide has been reported to induce small asperities on the surface,[6] and hence reaction progress can be imaged directly via SEM.

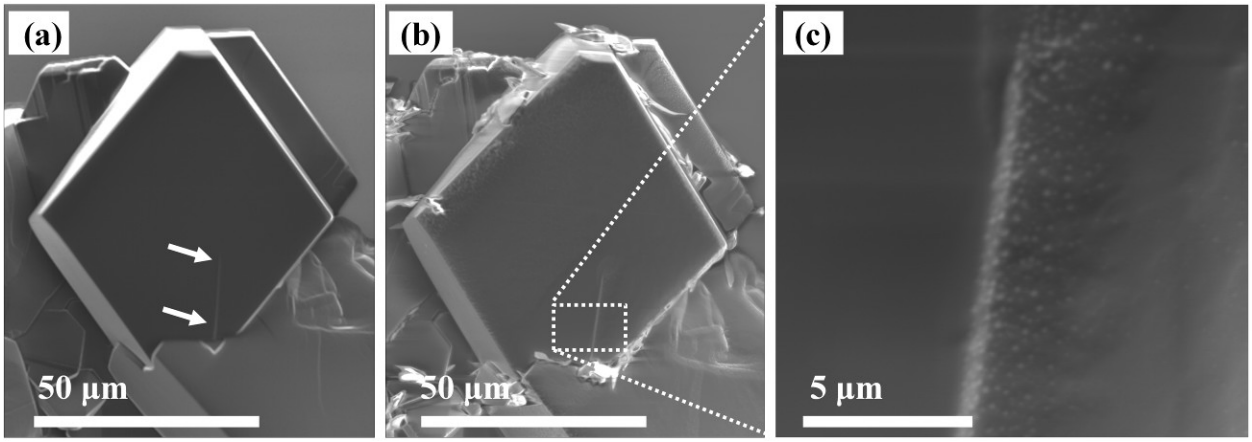

Figure 5. SEM images of tetracene crystals a) before reaction and b) after reaction with *N*-methylmaleimide. The white arrows indicate the dislocation defect on the surface. c) Magnified region displaying reaction propagation.

The crystals were exposed to *N*-methylmaleimide vapor at 80 °C for 18 h. The temperature was chosen based on prior evidence that the largest face of the tetracene crystals was inert at 80 °C.[8] The exposed crystals were re-examined with SEM to locate asperities indicative of reaction. Indeed, the images (Figure 5b and c) show adduct formation in the vicinity of the dislocation step, and importantly, the reaction appears to have propagated outward from the dislocation site. Analysis on additional tetracene crystals with dislocation defects demonstrate that this reaction propagation is representative (Figure S6). The reaction can be tracked as far as 3 ∝m from the nucleation site, with the product amount diminishing as a function of distance from the defect. Thus reactivity is not confined to the immediate vicinity of the defect. Additionally, the reaction's progression appears unidirectional (only to the right) from the defect. This is noteworthy as it suggests the adsorbate propagation initiates through the higher terrace within the dislocation. These results suggest that the defects not only play a role in the initiation of the reaction, but are also are important in the propagation of reaction.

CONCLUSIONS

In conclusion, the influence of defects on the reactivity of organic films was evaluated by performing the Diels-Alder reaction on what is nominally a pentacene (001) surface. By controlling defect density between samples via a temperature differential, reaction rates were correlated to higher defect density. In the context of previously reported inertness of a tetracene (001) surface, this reactivity indicates that defects are critical to reaction of this molecular orientation. This understanding was transitioned from a collection of defects to a direct observation of a single defect's influence on reactivity by studying reaction propagation from a dislocation in a single crystal. Results confirm the reaction is not confined to the immediate vicinity of the defect, but can propagate for microns across the crystal surface. Together, these results demonstrate the ability to react thin-film phase pentacene, and even the (001) surface of minimally flawed single crystals. These results represent a significant step towards improving the organic interface in top-contact OTFTs.

ASSOCIATED CONTENT

Supporting Information

Film deposition substrate stage with temperature calibration curve; temperature profile for the physical vapor transport tube furnace; additional AFM images of pentacene films; PM-IRRAS spectra of SAM absorptions in the ν_{CH} region; additional PM-IRRAS spectra of reacted pentacene films; additional SEM images of reaction propagation in tetracene crystals.

AUTHOR INFORMATION

Corresponding Author

E-mail: jciszek@luc.edu.

ORCID

Jixin Chen: 0000-0001-7381-0918

Jacob W. Ciszek: 0000-0002-6860-2900

Notes

The authors declare no competing financial interest.

ACKNOWLEDGMENTS

The authors gratefully acknowledge financial support from the National Science Foundation (NSF), Chemical Structure, Dynamic & Mechanism B Program of the Chemistry Division under Award No. 1665433. This research also utilized a scanning electron microscope, which was funded by the NSF, Major Research Instrumentation (MRI) Program via Award No. 1726994.

References

(1) Ma, H.; Yip, H.-L.; Huang, F.; Jen, A. K.-Y. Interface Engineering for Organic Electronics. *Adv. Funct. Mater.* **2010**, *20*, 1371–1388.
(2) Dennes, T. J.; Schwartz, J. A Nanoscale Metal Alkoxide/Oxide Adhesion Layer Enables Spatially Controlled Metallization of Polymer Surfaces. *ACS Appl. Mater. Interfaces* **2009**, *1*, 2119–2122.
(3) Braun, S.; Salaneck, W. R.; Fahlman, M. Energy-Level Alignment at Organic/Metal and Organic/Organic Interfaces. *Adv. Mater.* **2009**, *21*, 1450–1472.
(4) Hamadani, B. H.; Corley, D. A.; Ciszek, J. W.; Tour, J. M.; Natelson, D. Controlling Charge Injection in Organic Field-Effect Transistors Using Self-Assembled Monolayers. *Nano Lett.* **2006**, *6*, 1303–1306.

(5) Piranej, S.; Turner, D. A.; Dalke, S. M.; Park, H.; Qualizza, B. A.; Vicente, J.; Chen, J.; Ciszek, J. W. Tunable Interfaces on Tetracene and Pentacene Thin-Films via Monolayers. *CystEngComm* **2016**, *18*, 6062–6068.
(6) Deye, G. J.; Vicente, J. R.; Dalke, S. M.; Piranej, S.; Chen, J.; Ciszek, J. W. The Role of Thermal Activation and Molecular Structure on the Reaction of Molecular Surfaces. *Langmuir* **2017**, *33*, 8140–8146.
(7) Hu, W. S.; Tao, Y. T.; Hsu, Y. J.; Wei, D. H.; Wu, Y. S. Molecular Orientation of Evaporated Pentacene Films on Gold: Alignment Effect of Self-Assembled Monolayer. *Langmuir* **2005**, *21*, 2260–2266.
(8) Qualizza, B. A.; Prasad, S.; Chiarelli, M. P.; Ciszek, J. W. Functionalization of Organic Semiconductor Crystals via the Diels–Alder Reaction. *Chem. Commun.* **2013**, *49*, 4495–4497.
(9) Medveď, M.; Zoppellaro, G.; Ugolotti, J.; Matochová, D.; Lazar, P.; Pospíšil, T.; Bakandritsos, A.; Tuček, J.; Zbořil, R.; Otyepka, M. Reactivity of Fluorographene Is Triggered by Point Defects: Beyond the Perfect 2D World. *Nanoscale* **2018**, *10*, 4696–4707.
(10) Politano, A.; Chiarello, G.; Samnakay, R.; Liu, G.; Gürbulak, B.; Duman, S.; A. Balandin, A.; W. Boukhvalov, D. The Influence of Chemical Reactivity of Surface Defects on Ambient-Stable InSe-Based Nanodevices. *Nanoscale* **2016**, *8*, 8474–8479.
(11) Bikondoa, O.; Pang, C. L.; Ithnin, R.; Muryn, C. A.; Onishi, H.; Thornton, G. Direct Visualization of Defect-Mediated Dissociation of Water on TiO_2(110). *Nat. Mater.* **2006**, *5*, 189–192.
(12) Henrich, V. E.; Cox, P. A. *The Surface Science of Metal Oxides*; Cambridge University Press: Cambridge, 1994.
(13) Politano, A.; Chiarello, G.; Kuo, C.-N.; Lue, C. S.; Edla, R.; Torelli, P.; Pellegrini, V.; Boukhvalov, D. W. Tailoring the Surface Chemical Reactivity of Transition-Metal Dichalcogenide $PtTe_2$ Crystals. *Adv. Funct. Mater. 28*, 1706504.
(14) Cabrera-Sanfelix, P.; Darling, G. R. Dissociative Adsorption of Water at Vacancy Defects in Graphite. *J. Phys. Chem. C* **2007**, *111*, 18258–18263.
(15) Nickel, B.; Barabash, R.; Ruiz, R.; Koch, N.; Kahn, A.; Feldman, L. C.; Haglund, R. F.; Scoles, G. Dislocation Arrangements in Pentacene Thin Films. *Phys. Rev. B* **2004**, *70*, 125401.
(16) McCullough, J. D.; Curtin, D. Y.; Paul, I. C. Beckmann-Chapman Rearrangement in the Solid State of Oxime Picryl Ethers. *J. Am. Chem. Soc.* **1972**, *94*, 874–882.
(17) Cohen, M. D.; Ludmer, Z.; Thomas, J. M.; Williams, J. O. The Role of Structural Imperfections in the Photodimerization of 9-Cyanoanthracene. *Proc. R. Soc. Lond. Ser. A* **1971**, *324*, 459–468.
(18) Atwood, J. L.; Barbour, L. J.; Jerga, A.; Schottel, B. L. Guest Transport in a Nonporous Organic Solid via Dynamic van Der Waals Cooperativity. *Science* **2002**, *298*, 1000–1002.
(19) Laudise, R. A.; Kloc, C.; Simpkins, P. G.; Siegrist, T. Physical Vapor Growth of Organic Semiconductors. *J. Cryst. Growth* **1998**, *187*, 449–454.
(20) Seo, S.; Grabow, L. C.; Mavrikakis, M.; Hamers, R. J.; Thompson, N. J.; Evans, P. G. Molecular-Scale Structural Distortion near Vacancies in Pentacene. *Appl. Phys. Lett.* **2008**, *92*, 153313.

(21) Verlaak, S.; Rolin, C.; Heremans, P. Microscopic Description of Elementary Growth Processes and Classification of Structural Defects in Pentacene Thin Films. *J. Phys. Chem. B* **2007**, *111*, 139–150.
(22) Seo, S.; Evans, P. G. Molecular Structure of Extended Defects in Monolayer-Scale Pentacene Thin Films. *J. Appl. Phys.* **2009**, *106*, 103521.
(23) Lee, H. S.; Kim, D. H.; Cho, J. H.; Hwang, M.; Jang, Y.; Cho, K. Effect of the Phase States of Self-Assembled Monolayers on Pentacene Growth and Thin-Film Transistor Characteristics. *J. Am. Chem. Soc.* **2008**, *130*, 10556–10564.
(24) Bock, C.; Pham, D. V.; Kunze, U.; Käfer, D.; Witte, G.; Wöll, C. Improved Morphology and Charge Carrier Injection in Pentacene Field-Effect Transistors with Thiol-Treated Electrodes. *J. Appl. Phys.* **2006**, *100*, 114517.
(25) Kim, D. H.; Lee, H. S.; Yang, H.; Yang, L.; Cho, K. Tunable Crystal Nanostructures of Pentacene Thin Films on Gate Dielectrics Possessing Surface-Order Control. *Adv. Funct. Mater. 18*, 1363–1370.
(26) Celle, C.; Suspène, C.; Ternisien, M.; Lenfant, S.; Guérin, D.; Smaali, K.; Lmimouni, K.; Simonato, J. P.; Vuillaume, D. Interface Dipole: Effects on Threshold Voltage and Mobility for Both Amorphous and Poly-Crystalline Organic Field Effect Transistors. *Org. Electron.* **2014**, *15*, 729–737.
(27) Hill, I. G.; Weinert, C. M.; Kreplak, L.; Zyl, B. P. van. Influence of Self-Assembled Monolayer Chain Length on Modified Gate Dielectric Pentacene Thin-Film Transistors. *Appl. Phys. A* **2009**, *95*, 81–87.
(28) Fukuda, K.; Hamamoto, T.; Yokota, T.; Sekitani, T.; Zschieschang, U.; Klauk, H.; Someya, T. Effects of the Alkyl Chain Length in Phosphonic Acid Self-Assembled Monolayer Gate Dielectrics on the Performance and Stability of Low-Voltage Organic Thin-Film Transistors. *Appl. Phys. Lett.* **2009**, *95*, 203301.
(29) Acton, B. O.; Ting, G. G.; Shamberger, P. J.; Ohuchi, F. S.; Ma, H.; Jen, A. K.-Y. Dielectric Surface-Controlled Low-Voltage Organic Transistors via n-Alkyl Phosphonic Acid Self-Assembled Monolayers on High-k Metal Oxide. *ACS Appl. Mater. Interfaces* **2010**, *2*, 511–520.
(30) Lang, P.; Mottaghi, D.; Lacaze, P.-C. On the Relationship between the Structure of Self-Assembled Carboxylic Acid Monolayers on Alumina and the Organization and Electrical Properties of a Pentacene Thin Film. *Appl. Surf. Sci.* **2016**, *365*, 364–375.
(31) Pratontep, S.; Brinkmann, M.; Nüesch, F.; Zuppiroli, L. Nucleation and Growth of Ultrathin Pentacene Films on Silicon Dioxide: Effect of Deposition Rate and Substrate Temperature. *Synth. Met.* **2004**, *146*, 387–391.
(32) Venables, J. A.; Spiller, G. D. T.; Hanbucken, M. Nucleation and Growth of Thin Films. *Rep. Prog. Phys.* **1984**, *47*, 399–459.
(33) Stadlober, B.; Haas, U.; Maresch, H.; Haase, A. Growth Model of Pentacene on Inorganic and Organic Dielectrics Based on Scaling and Rate-Equation Theory. *Phys. Rev. B* **2006**, *74*, 165302.
(34) Kalihari, V.; Tadmor, E. B.; Haugstad, G.; Frisbie, C. D. Grain Orientation Mapping of Polycrystalline Organic Semiconductor Films by Transverse Shear Microscopy. *Adv. Mater. 20*, 4033–4039.
(35) Minakata, T.; Imai, H.; Ozaki, M.; Saco, K. Structural Studies on Highly Ordered and Highly Conductive Thin Films of Pentacene. *J. Appl. Phys.* **1992**, *72*, 5220–5225.

(36) Porter, M. D.; Bright, T. B.; Allara, D. L.; Chidsey, C. E. D. Spontaneously Organized Molecular Assemblies. 4. Structural Characterization of n-Alkyl Thiol Monolayers on Gold by Optical Ellipsometry, Infrared Spectroscopy, and Electrochemistry. *J. Am. Chem. Soc.* **1987**, *109*, 3559–3568.
(37) Pensa, E.; Cortés, E.; Corthey, G.; Carro, P.; Vericat, C.; Fonticelli, M. H.; Benítez, G.; Rubert, A. A.; Salvarezza, R. C. The Chemistry of the Sulfur–Gold Interface: In Search of a Unified Model. *Acc. Chem. Res.* **2012**, *45*, 1183–1192.
(38) Laibinis, P. E.; Whitesides, G. M.; Allara, D. L.; Tao, Y. T.; Parikh, A. N.; Nuzzo, R. G. Comparison of the Structures and Wetting Properties of Self-Assembled Monolayers of n-Alkanethiols on the Coinage Metal Surfaces, Copper, Silver, and Gold. *J. Am. Chem. Soc.* **1991**, *113*, 7152–7167.
(39) Griffiths, P. R.; De Haseth, J. A. *Fourier Transform Infrared Spectrometry*, 2nd ed.; Chemical analysis; Wiley-Interscience: Hoboken, N.J, 2007.

TOC Graphic